Journal of Engineering Mathematics (2006) 54: 89–97
DOI 10.1007/s10665-005-7719-9

Truncation approximations for gravity-capillary free-surface flows

S. GRANDISON and J.-M. VANDEN-BROECK
School of Mathematics, University of East Anglia, Norwich NR4 7TJ, England (s.grandison@uea.ac.uk)

Received 26 November 2004; accepted in revised form 4 May 2005

Abstract. Gravity-capillary free-surface flows past disturbances in a channel of finite depth are considered. These flows are usually assumed to extend from $x=-\infty$ to $x=\infty$ where the x-axis is parallel to the bottom. Many numerical schemes truncate this infinite domain to the interval $-B<x<A$ where A and B are large positive numbers. These truncations introduce inaccuracies, especially when the effect of surface tension is included. In this paper numerical methods are presented which remove these inaccuracies. This is achieved by taking into account the contributions from $-\infty$ to $-B$ and from A to ∞. Explicit computations are presented for a semi-circular obstacle at the bottom of the channel.

Key words: boundary-integral-equation methods, free-surface flows, gravity-capillary waves

1. Introduction

Many two-dimensional potential free-surface flows occurring in hydrodynamics possess trains of periodic waves in the far field. One example is the gravity-capillary free-surface flow generated by disturbances moving at a constant velocity in a channel of finite depth. The disturbance can be a submerged object (modelling a submarine), a surface piercing object (modelling a ship) or a distribution of pressure with a compact support.

When the disturbance is small, the equations can be linearised and an analytical solution can be derived by Fourier transforms (see [1, pp. 384–413]). On the other hand, for large disturbances, no analytical solutions are available and the fully nonlinear equations have to be solved numerically. This can be achieved efficiently by using boundary-integral-equation methods [2–8]. One difficulty is that the free surface is unbounded in the horizontal direction. Therefore it extends from $x=-\infty$ to $x=+\infty$ where the x-axis is parallel to the bottom.

To solve the problem numerically it is necessary to truncate it at $x=-B$ and $x=A$ where A and B are large positive numbers. As we shall see, the potential function ϕ is often used as an independent variable. In such a case the domain is truncated at $\phi=-t_1$ and $\phi=t_2$ where t_1 and t_2 are large positive numbers. These truncations can generate numerical inaccuracies. In this paper we derive new truncation approximations which minimise these inaccuracies.

The results presented are qualitatively independent of the form of the disturbance. Here we assume that the disturbance is a submerged semi-circular cylinder moving at a constant velocity at the bottom of a channel (see Figure 1). This problem was considered before by Forbes and Schwartz [3], Forbes [4] and Vanden-Broeck [6]. We take a frame of reference moving with the disturbance. The flow is assumed to be to the right (*i.e.*, from $x=-\infty$ to $x=\infty$). We restrict our attention to steady solutions. We also concentrate on flows for which there are trains of waves on the free surface because they are more sensitive to truncations than flows with waveless flat free surfaces in the far field.

When surface tension is neglected, the free surface is flat at large distances in front of the disturbance and may possess a train of waves a large distance behind the obstacle. The work

of Forbes and Schwartz [3] shows that it is possible to obtain accurate nonlinear numerical solutions by simply neglecting in the boundary-integral-equation formulation the contributions to the integrals from $x=-\infty$ to $x=-A$ and from $x=B$ to $x=\infty$. There are, however, small spurious waves a large distance in front of the obstruction (*i.e.*, for $x<0$) and a distortion in the last wavelength of the train of waves (see Figures in [4]). We show that our improved truncation reduces greatly the amplitude of the spurious waves.

When surface tension is taken into account, the situation is much more complicated. Firstly, there are in general trains of waves both at the front and at the back of the disturbance. The numerical inaccuracy in the downstream waves resulting from truncating the domain is restricted to approximately the last wavelength of the flow. Upstream inaccuracies caused by truncation are even more dramatic with large-amplitude spurious waves of the same wavelength as the downstream waves and a constantly decreasing mean free-surface elevation. The results presented by Forbes [4] show a free surface with a constantly decreasing mean height. We shall present numerical methods to remove these inaccuracies.

The problem in the absence of surface tension is formulated in Section 2. The numerical procedure and the techniques to remove the inaccuracies are described in Section 3. The problems with surface tension are considered in Section 4.

2. Formulation

Let us consider the steady flow over a semi-circular obstacle of radius R at the bottom of a channel (see Figure 1). We introduce Cartesian co-ordinates with the x-axis along the bottom and the origin at the centre of the semi-circular obstacle. The gravity g is acting in the negative y-direction. When surface tension is neglected, the flow approaches a uniform stream as $x\to-\infty$ with a constant velocity U and constant depth H. We introduce dimensionless variables by taking H as the unit length and U as the unit velocity.

We then define the following complex variables $z=x+\mathrm{i}y$, the complex potential $f=\phi+\mathrm{i}\psi$, and the complex velocity $u-\mathrm{i}v$. Without loss of generality we choose $\psi=0$ on the bottom, so that $\psi=1$ on the free surface. The condition of constant pressure on the free surface can be written

$$\frac{1}{2}F^2(u^2+v^2)+y=\frac{1}{2}F^2+1. \tag{1}$$

Here F is the Froude number defined by

$$F=\frac{U}{(gH)^{1/2}}. \tag{2}$$

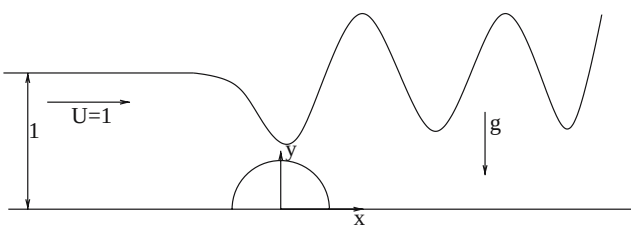

Figure 1. Sketch of the flow configuration. When the surface tension is neglected, the free surface is flat as $x\to-\infty$ and wavy as $x\to\infty$. When the surface tension is taken into account, there is in addition a train of waves as $x\to-\infty$. The sketch corresponds to the case without surface tension.

Following Forbes and Schwartz [3], we define the new variable $\zeta = \xi + \mathrm{i}\eta$ by the relation

$$\xi + \mathrm{i}\eta = \frac{1}{2}\left(z + \frac{\alpha^2}{z}\right), \tag{3}$$

where $\alpha = R/H$ is the dimensionless radius of the semi-circle.

Relation (3) is the classical Joukowskii transformation; it maps the z-plane into a ζ-plane in which the bottom streamline is a straight line. We shall seek $\xi + \mathrm{i}\eta$ as an analytic function of $f = \phi + \mathrm{i}\psi$ in the strip $0 < \psi < 1$. In terms of the variable $\zeta(\phi, \psi)$, Equation (1) becomes

$$F^2 \frac{(z^2 - \alpha^2)(\bar{z}^2 - \alpha^2)}{8(z\bar{z})^2 \zeta_\phi \overline{\zeta_\phi}} + \mathfrak{Im}[z] - \frac{1}{2}F^2 - 1 = 0, \tag{4}$$

where the bar signifies the complex conjugate and $\mathfrak{Im}$ denotes the imaginary part.

By using Cauchy integral-equation formula, Forbes and Schwartz [3] derived the following integral relation between $\xi(\phi, 1)$ and $\eta(\phi, 1)$:

$$\left[\xi_\phi(\phi, 1) - \frac{1}{2}\right] - \frac{2}{\pi}\int_{-\infty}^{+\infty}\left[\xi_\phi(\theta, 1) - \frac{1}{2}\right]\frac{\mathrm{d}\theta}{(\theta - \phi)^2 + 4}$$

$$= -\frac{1}{\pi}\left\{\int_{-\infty}^{+\infty}\frac{\eta_\theta(\theta, 1)(\theta - \phi)}{(\theta - \phi)^2 + 4}\mathrm{d}\theta + \int_{-\infty}^{+\infty}\frac{\eta_\theta(\theta, 1)}{(\theta - \phi)}\mathrm{d}\theta\right\}. \tag{5}$$

The second integral on the right-hand side of the equation is a Cauchy principal value.

This concludes the formulation of the problem. For given values of α and F, we seek two functions ξ and η satisfying (4) and (5).

3. Free-surface flows without surface tension

We describe in Section 3.1 the basic numerical procedure in which the integrals from $-\infty$ to ∞ in (5) are truncated at finite values. Then in Section 3.2 we present an improved scheme in which the integrals are not truncated.

3.1. Results with truncation of the integrals

The numerical method follows closely the work of Forbes and Schwartz [3] and of Forbes [4]. The reader is referred to those papers for details.

We first truncate the three integrals from $-\infty$ to ∞ in (5) to integrals from $-t_1$ to t_2 where t_1 and t_2 are large positive numbers. Then we define equally spaced points

$$\phi_I = -t_1 + \frac{t_2 + t_1}{N} I, \quad I = 0, \ldots, N,$$

and the corresponding unknowns

$$\xi'_I = \xi_\phi(\phi_I, 1), \quad I = 0, \ldots, N,$$
$$\eta'_I = \eta_\phi(\phi_I, 1), \quad I = 0, \ldots, N.$$

The problem is then discretised. In particular, the integrals are approximated by the trapezoidal rule or by the Simpson rule. Relations (4) and (5) yield a system of nonlinear algebraic equations for the unknowns ξ'_I and η'_I. This system is solved by Newton iterations. The radiation condition in the absence of surface tension is equivalent to the requirement that the free

surface profile is flat as $x \to -\infty$. This is imposed by forcing $\eta = 1/2$ and $\eta_\phi = 0$ at the first mesh point ϕ_0.

The above numerical scheme gives very good results (see [3] for examples). However, as noted by Forbes and Schwartz, spurious small waves appear in front of the obstacle (*i.e.*, in the region $x < 0$). These waves do not satisfy the radiation condition and are an artifact of the numerical procedure. There is also a distortion in approximately the last quarter wavelength of the downstream waves, which, although insignificant, can prevent the numerical method from converging at large values of the Froude number.

We present in the next Section a numerical method which improves the accuracy, removes the spurious waves and reduces the distortion.

3.2. Results without truncation of the integrals

The inaccuracies in the scheme of Section 3.1 are caused by the replacements of the integrals from $-\infty$ to ∞ in (5) by integrals from $\phi = -t_1$ to $\phi = t_2$.

We shall show that these inaccuracies are greatly reduced by including suitable approximations of the integrals from $-\infty$ to $-t_1$ and from t_2 to ∞.

We consider first the integrals from $-\infty$ to $-t_1$. As $\phi \to -\infty$, the flow approaches a uniform stream with velocity 1. We derive in the Appendix the general form of a perturbed uniform stream with a free surface. Using the facts that $\phi \approx x$ and $y \approx 2\eta$ as $\phi \to -\infty$, we obtain from (A.14)

$$\eta_\phi \approx A e^{\lambda \phi} \quad \text{as } \phi \to -\infty, \tag{6}$$

where A is a constant and λ is the smallest positive root of

$$\lambda - \frac{\tan \lambda}{F^2} = 0. \tag{7}$$

We then obtain

$$\xi_\phi \approx C \quad \text{as } \phi \to -\infty, \tag{8}$$

where C is a constant.

We now use (8) and (6) to approximate the three integrals from $-\infty$ to $-t_1$

$$\int_{-\infty}^{-t_1} \left[\xi_\phi(\theta, 1) - \frac{1}{2} \right] \frac{d\theta}{(\theta - \phi)^2 + 4} \approx \left[C - \frac{1}{2} \right] \left[\frac{1}{2} \arctan \frac{-(t_1 + \phi)}{2} + \frac{\pi}{4} \right], \tag{9}$$

$$\int_{-\infty}^{-t_1} \frac{\eta_\theta(\theta, 1)(\theta - \phi)}{(\theta - \phi)^2 + 4} d\theta \approx A \int_{-\infty}^{-t_1} \frac{e^{\lambda\theta}(\theta - \phi)}{(\theta - \phi)^2 + 4} d\theta, \tag{10}$$

$$\int_{-\infty}^{-t_1} \frac{\eta_\theta(\theta, 1)}{\theta - \phi} d\theta \approx A \int_{-\infty}^{-t_1} \frac{e^{\lambda\theta}}{\theta - \phi} d\theta. \tag{11}$$

The constants A and C are found by requiring that (6) and (8) are satisfied at the last mesh point ϕ_N.

We now consider the integrals from t_2 to ∞. This is more complicated than the previous case because there are nonlinear waves on the free surface for $\phi > 0$. However, the waves ultimately approach a train of periodic waves as $\phi \to \infty$. Therefore we assume that the waves repeat themselves without change of shape or amplitude for $\phi > t_2$. This is a good approximation for t_2 large. We define at each iteration two values $p_1 < p_2$ of ϕ which correspond to

the two crests of the train of waves closest to $\phi = t_2$ (*i.e.*, the two crests further on the right in Figure 1). We define η_ϕ for $\phi > t_2$ by

$$\eta_\phi(t_2 + s) = \eta_\phi(t_2 + p_1 - p_2 + s) \quad \text{for } s < p_2 - p_1 \tag{12}$$

and more generally

$$\eta_\phi(t_2 + s) = \eta_\phi[t_2 + p_1 - p_2 + s - n(p_2 - p_1)] \quad \text{for } n(p_2 - p_1) < s < (n+1)(p_2 - p_1). \tag{13}$$

Here $s > 0$ and n is a positive integer.

Similarly we write

$$\xi_\phi(t_2 + s) = \xi_\phi[t_2 + p_1 - p_2 + s - n(p_2 - p_1)] \quad \text{for } n(p_2 - p_1) < s < (n+1)(p_2 - p_1). \tag{14}$$

We approximate the integrals from t_2 to ∞ by summations using the trapezoidal rule, thus

$$\int_{t_2}^{\infty} \left[\xi_\phi(\theta, 1) - \frac{1}{2}\right] \frac{\mathrm{d}\theta}{(\theta - \phi)^2 + 4} \approx \sum_{n=1}^{N_{\max}} \sum_{s=p_1}^{p_2} h \frac{\xi_\phi[s] - \frac{1}{2}}{(\theta_s + h(p_2 - p_1)(n-1) - \phi)^2 + 4}, \tag{15}$$

$$\int_{t_2}^{\infty} \frac{\eta_\theta(\theta, 1)(\theta - \phi)}{(\theta - \phi)^2 + 4} \mathrm{d}\theta \approx \sum_{n=1}^{N_{\max}} \sum_{s=p_1}^{p_2} h \frac{\eta_\phi[s](\theta_s + h(n-1) - \phi)}{(\theta_s + h(p_2 - p_1)(n-1) - \phi)^2 + 4}, \tag{16}$$

$$\int_{t_2}^{\infty} \frac{\eta_\theta(\theta, 1)}{(\theta - \phi)} \mathrm{d}\theta \approx \sum_{n=1}^{N_{\max}} \sum_{s=p_1}^{p_2} h \frac{\eta_\phi[s]}{\theta_s + h(p_2 - p_1)(n-1) - \phi}, \tag{17}$$

where h is the separation between mesh points and $N_{\max} >> 1$.

Relations (12–14) define η_ϕ and ξ_ϕ for $\phi > t_2$ in terms of their values for $\phi < t_2$. This enables us to extend the trapezoidal (or Simpson) rule approximation of the integrals in (2.5) to values of ϕ much larger than t_2 without introducing extra unknown ξ_I and η_I or increasing significantly the computing time. Figure 2 shows a typical free-surface profile. We note the elimination of waves upstream of the disturbance. Figure 3 shows the upstream surface in more detail. All results presented were obtained with $N = 300$ mesh points. We checked that these results are correct within graphical accuracy by varying N.

Making the above downstream approximation removes the distortion in the last quarter wavelength experienced by Forbes and Schwartz [3], and allows us to compute solutions for flow speeds greater than that computed by these authors. Convergence was obtained for values of the Froude number up to $F = 0{\cdot}555$, for $\alpha = 0{\cdot}2$ (see Figure 4), which is close to the maximum flow speed of $F = 0{\cdot}6$, conjectured by [3] where wave-like solutions might be found.

The profile of Figure (4) contains highly nonlinear waves with sharp crests and broad troughs. This profile demonstrates that the radiation condition is effectively satisfied and that there is no downstream distortion.

4. Free surface flows with surface tension

When surface tension is included the kinematic boundary condition remains unchanged but the dynamic boundary condition becomes

$$\frac{1}{2}F^2(u^2 + v^2) + y - WK = \frac{1}{2}F^2 + 1, \tag{18}$$

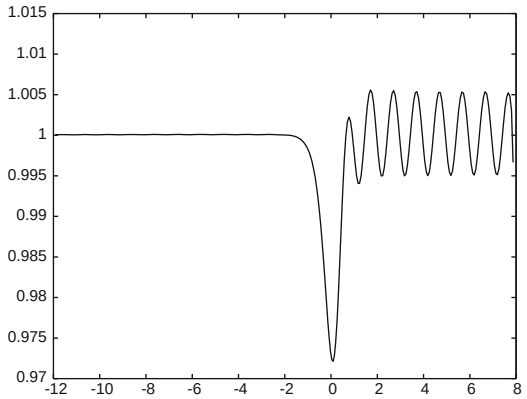

Figure 2. Free-surface flow for $\alpha = 0{\cdot}2$, $F = 0{\cdot}4$.

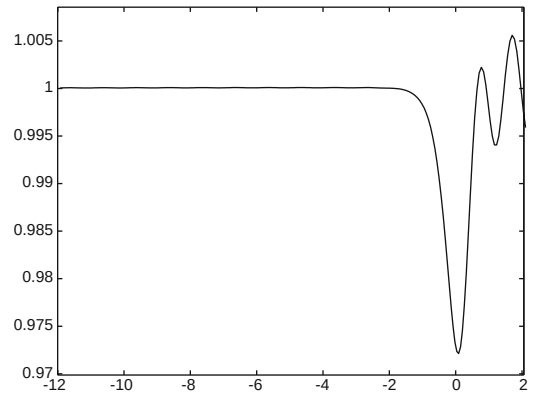

Figure 3. Free-surface flow for $\alpha = 0{\cdot}2$, $F = 0{\cdot}4$. The upstream free-surface is shown in more detail to highlight the absence of waves.

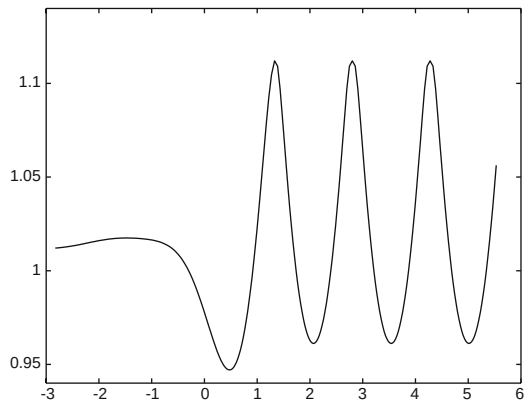

Figure 4. Free-surface flow for $\alpha = 0{\cdot}2$, $F = 0{\cdot}555$.

where K is the local curvature at the free surface and W is the Weber Number defined by

$$W = \frac{T}{\rho g H^2}.$$

Here T is the surface tension.

Following Forbes [4] we obtain

$$\frac{1}{8}F^2\frac{(z^2-\alpha^2)(\bar{z}^2-\alpha^2)}{(z\bar{z})^2(\zeta_\phi\bar{\zeta}_\phi)} + \Im\mathfrak{m}[z] - \frac{1}{2}F^2 - 1 - \frac{1}{4}\mathrm{i}T\frac{(z^2-\alpha^2)^{\frac{1}{2}}(\bar{z}^2-\alpha^2)^{\frac{1}{2}}}{(z\bar{z})(\zeta_\phi\bar{\zeta}_\phi)^{\frac{3}{2}}}\left[(\zeta_\phi\bar{\zeta}_{\phi\phi} - \bar{\zeta}_\phi\zeta_{\phi\phi}) + 4\alpha^2(\zeta_\phi\bar{\zeta}_\phi)\left[\frac{z\zeta_\phi}{(z^2-\alpha^2)^2} - \frac{\overline{z\zeta_\phi}}{(\bar{z}^2-\alpha^2)^2}\right]\right] = 0. \tag{19}$$

This expression is similar to (4) but contains an extra term which relates to the curvature at the free surface.

When surface tension is included, there are in general trains of waves both upstream and downstream. We use the method described in Section (3.2) to approximate the integrals from t_2 to $+\infty$. The method used in Section 3.2 to approximate the integral from $-\infty$ to $-t_1$ is

no longer applicable because of the upstream train of waves. Here we use a generalisation of the approach developed by Vanden-Broeck [9] to calculate Wilton's ripples.

Vanden-Broeck's approach consists of approximating η_ϕ in $-\infty < \phi < A$ by

$$\eta_\phi = D\sin(k\phi + \omega), \tag{20}$$

where D, k and θ have to be found as part of the solution.

Relation (20) approximates the waves in $-\infty < \phi < A$ by linear waves. It is therefore a good approximation if these waves are of small amplitude.

An extension of (20) consists of writing

$$\eta_\phi = \sum_{n=1}^{N} D_n \sin(nk\phi + \theta). \tag{21}$$

Relation (21) is now an approximation for nonlinear waves and is exact in the limit $N \to \infty$. The constants $D_1, D_2, \ldots, D_N$, k and θ are found by fitting values of η_ϕ at points on the discretised mesh close to A.

We repeated the calculations for different values of N and checked that the results presented are independent of N.

This truncation procedure enables us to confirm and improve the results of Forbes [4]. The results presented by Forbes do not have a constant mean upstream height and the upstream wavelength is also too high. Furthermore the distortion that occurs in the $T = 0$ case is even more pronounced in the $T \neq 0$ case and extends over two wavelengths.

In Figure 5 we present results in the absence of surface tension to contrast them to the gravity-capillary solution of Figure 6. As can be seen in Figure 6 the modified model not only demonstrates the existence of a solution with a train of waves both upstream and downstream but the previous problems associated with this computation, namely the decreasing mean height of the upstream waves and the violation of the radiation condition has been eliminated. Linear theory predicts an upstream wavelength of $\lambda \approx 0{\cdot}8796$ and a downstream wavelength of $\lambda \approx 3{\cdot}4247$; these predictions agree to within 2% of the full numerical scheme.

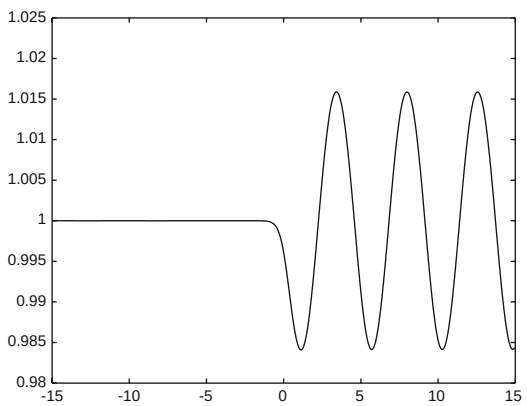

Figure 5. Free-surface flow for $\alpha = 0{\cdot}05$, $F = 0{\cdot}8$, $W = 0$.

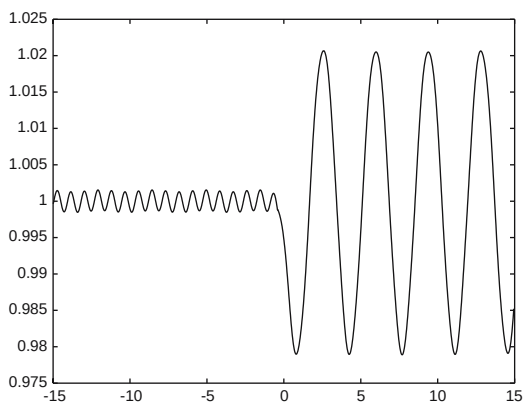

Figure 6. Free-surface flow for $\alpha = 0{\cdot}05$, $F = 0{\cdot}8$, $T = 0{\cdot}07$.

5. Discussion

A numerical model for free-surface flow over a semicircular obstacle, based on the work of Forbes and Schwartz [3] has been investigated. We solved the exact nonlinear equations using the complex potential f rather than physical co-ordinates; this has the advantage of transforming the problem into a frame where the free surface is known. The model is further developed by choosing a conformal mapping to eliminate singularities along the bottom of the channel. The nonlinear equations are then discretised by means of the trapezoidal rule and solved by a modified Newtonian iteration scheme.

Inaccuracies in previous models, namely the violation of the radiation condition and the distortion of downstream waves close to the point of truncation have been eliminated by use of appropriate approximations of the flow far upstream and downstream of the obstacle.

These approximations are general and can be used for any gravity-capillary free-surface flow past a disturbance.

Acknowledgements

This work was supported by the Norwich Research Park and EPSRC

Appendix A. Far-field solution

In this appendix, we derive briefly the solution for the perturbation of a uniform stream with constant velocity U and constant depth H. The flow domain is bounded above by a free surface and below by a horizontal bottom.

The exact equations are

$$\phi_{xx} + \phi_{yy} = 0, \tag{A.1}$$

$$\phi_y = \phi_x f_x \quad \text{on } y = f(x), \tag{A.2}$$

$$\frac{\phi_x^2 + \phi_y^2}{2} + gf = \frac{U^2}{2} + gH \quad \text{on } y = f(x), \tag{A.3}$$

$$\phi_y = 0 \quad \text{on } y = 0. \tag{A.4}$$

Here $\phi(x, y)$ is the potential function, g is the acceleration of gravity and $y = f(x)$ is the equation of the free surface. We now write

$$\phi(x, y) = Ux + \varphi(x, y), \tag{A.5}$$

$$f(x) = H + h(x), \tag{A.6}$$

where $\varphi(x, y)$ and $h(x)$ are assumed to be small perturbations.

Substituting (A.5) and (A.6) in (A.1–A.4) and keeping only the terms linear in φ and h yields

$$\varphi_{xx} + \varphi_{yy} = 0, \tag{A.7}$$

$$\varphi_y = Uh_x \quad \text{on } y = H, \tag{A.8}$$

$$U\varphi_x + gh = 0 \quad \text{on } y = H, \tag{A.9}$$

$$\varphi_y = 0 \quad \text{on } y = 0. \tag{A.10}$$

Eliminating h between (A.9) and (A.10) gives

$$U^2\varphi_{xx} + g\varphi_y = 0. \tag{A.11}$$

Solving (A.7) by separations of variables and using (A.10) yield

$$\varphi = B\mathrm{e}^{\beta x}\cos\beta y. \tag{A.12}$$

Here B and β are constants. We assume that $\beta < 0$ when $x > 0$ and that $\beta > 0$ when $x < 0$, so that the flow reduces to a uniform stream as $|x| \to \infty$.

Substituting (A.12) in (A.11) yields

$$F^2\beta H = \tan\beta H, \tag{A.13}$$

Finally a substitution of (A.12) in (A.8) gives after integration

$$h(x) = D\mathrm{e}^{\beta x}, \tag{A.14}$$

where D is a constant.

References

1. H. Lamb, *Hydrodynamics*. Cambridge: Cambridge University Press (1945) 730 pp.
2. J.-M. Vanden-Broeck, Nonlinear stern waves. *J. Fluid Mech.* 96 (1980) 601–610.
3. L.K. Forbes and L.W. Schwartz, Free-surface flow over a semicircular obstruction. *J. Fluid Mech.* 114 (1982) 299–314.
4. L.K. Forbes, Free-surface flow over a semicircular obstruction, including the influence of gravity and surface tension. *J. Fluid Mech.* 127 (1983) 283–297.
5. J. Asavanant and J.-M. Vanden-Broeck, Free-surface flows past a surface piercing object of finite length. *J. Fluid Mech.* 273 (1994) 109–124.
6. J.-M. Vanden-Broeck, Free-surface flow over an obstruction in a channel. *Phys. Fluids* 30 (1987) 2315–2317.
7. A. C. King and M. I. G. Bloor, Free-surface flows over a step. *J. Fluid Mech.* 182 (1987) 193–208.
8. D. Scullen and E. O. Tuck, Nonlinear free-surface flow computations for a submerged cylinder. *J. Ship Res.* 39 (1995) 185–193.
9. J.-M. Vanden-Broeck, Wilton ripples generated by a moving pressure distribution. *J. Fluid Mech.* 451 (2002) 193–201.